Progress of Theoretical Physics, Vol. 59, No. 3, March 1978

Flow Patterns of Cluster Winds and X-Ray Emissions from Clusters of Galaxies

Yuzo HIRAYAMA, Yasuo TANAKA* and Tomokazu KOGURE**

Department of Physics, Hokkaido University, Sapporo 060
**Faculty of Education, Ibaraki University, Mito 310*
***Department of Astronomy, Kyoto University, Kyoto 606*

(Received September 8, 1977)

The flow of intracluster gas injected from galaxies by galactic winds or ram pressure is investigated by numerical time-dependent calculations in the beam scheme.

Under a given gravitational field and mass loss rate, there are three flow patterns at the Hubble time, depending on the temperature of the injected gas. If we take a gravitational field of the Coma cluster, lower temperature of the injected gas than 10^6 °K and higher temperature than 3×10^8 °K result in wholly inward and wholly outward flow, respectively. For the temperature between them, there appears a partially inward and outward flow that the injected gas flows inwardly within a stagnation point and outwardly outside of it.

The highest X-ray luminosity is expected for the case of the pure inflows, because of high central gas density. The pure outflows become steady at the Hubble time and result in the lowest luminosity in spite of higher central temperatures. The partial flows are the intermediate case. It is concluded that the results for the pure inflow or partial flow models are consistent with X-ray observational data of the Coma cluster.

§ 1. Introduction

Many clusters of galaxies are known as powerful X-ray sources[1] and models of X-ray emissions from these clusters have been proposed. There are two types of the models, that is, the thermal bremsstrahlung model and the inverse-Compton model. However, observations of X-ray spectra and of iron line emissions at 7 keV from clusters[2),3)] seem to support the existence of a hot intracluster plasma with a temperature of 10^8 °K and favor the thermal bremsstrahlung model. The iron line emission also suggests that the hot plasma might be supplied not only from primordial matter left at the initial formation of galaxies but also from stars in galaxies where the nuclear synthesis proceeded.

Gull and Northover[4] and Lea[5] studied static models of hot primordial matter. They and other authors[6] computed the infall of the primordial gas or the intracluster gas distributed homogeneously. They, however, ignored the effect of the gas ejected from stars in galaxies into clusters.

The theory of stellar evolution reveals that a part of stellar mass is shedded into galaxies when less massive stars evolve from the giant branch to the horizontal branch,[7] while observations directly show that mass loss from stars occurs as planetary nebula and supernova. It is also likely that the stellar winds from various types of stars and mass loss from flare stars[8] add gas to interstellar matter. The fate of the ejected gas is argued by several authors. Mathews and Baker[9] showed that in a typical elliptical galaxy the ejected gas flows outwardly if supernovae supply sufficient energy. Ipavich[10] argued that cosmic rays give rise to the outward galactic winds in ellipticals. Steady wind solutions were analysed by Johnson and Axford[11] who pointed out the possibility of outward flow, inward flow and partially inward and outward flow that the injected gas flows inwardly within a stagnation point and outwardly outside of it. It is expected that if the stagnation point of the partial flow locates near the center of the galaxy, most of the ejected gas from stars flows out of the galaxy. In addition to the galactic winds, the injection into the intracluster space is possible by the stripping of gas from galaxies moving in dense gaseous matter.[12] In clusters of galaxies, there may be a primordial gas left at the formation of galaxies and/or gas injected from galaxies. Lea and De Young[13] calculated in detail the distribution of the density, temperature and velocity of the gas stripped from a model galaxy. Both mechanisms cause the injection of the ejected gas from stars in galaxies into the intracluster space.

Although Yahil and Ostriker[14] studied outflow models in clusters of galaxies and obtained steady solutions, they were forced to assume huge heat supply for the interpretation of the observed X-ray luminosity of the Coma cluster.

In the present work, we study numerically time-dependent behavior of the injected gas in clusters of galaxies as an extension of the work by Johnson and Axford.[11] Subsequent to the completion of our calculation, numerical time-dependent solutions of the injected intracluster gas were obtained by Cowie and Perrenod[15] who argued the evolution of X-ray sources over cosmological time scales. Cowie and Binney[16] also studied steady inflow models on the assumption of self-regulation at the central part. However, they discussed only the solutions of inflows, assuming a rather low temperature of injected gas.

In § 2 we show the basic equations and our choice of non-dimensional parameters which determine the characteristics of flows. Fixing gravitational fields and mass loss rates, we calculate flows for various temperatures of the injected gas. In § 3 the time variations of distributions of physical quantities are obtained and flow patterns are classified by the temperature of the injected gas. The quantities relevant to X-ray observational data are also obtained. The results are discussed in comparison with the case of infall of primordial gas. It is shown in § 4 that the observational X-ray data of the Coma cluster are consistent with the present results for the cases of wholly inward flow and partial flow.

§ 2. Models and assumptions

According to King,[17] the spherical density distribution of galaxies in a cluster is written as

$$\rho_*(r)=\rho_*(0)/(1+r^2/b^2)^{1.5}\,, \tag{1}$$

where r is the radius from the center, $\rho_*(0)$ the density of galaxies at the center and b the core radius of the cluster. The mass of galaxies within the radius r is obtained by integration of Eq. (1) as

$$M_*(r)=3M_c\left[\ln\left\{\frac{r}{b}+\left(1+\frac{r^2}{b^2}\right)^{0.5}\right\}-\frac{r/b}{(1+r^2/b^2)^{0.5}}\right], \tag{2}$$

where the core mass M_c is defined by $4\pi b^3\rho_*(0)/3$. In numerical calculations, we adopt the following values of the Coma cluster[18] for $\rho_*(0)$, b and the total mass of galaxies in the cluster $M_*(6.5\,\mathrm{Mpc})$, taking the Hubble constant equal to 50 km sec^{-1} Mpc^{-1}:

$$\rho_*(0)=4.55\times10^{-3}M_\odot/\mathrm{pc}^3\,,$$

$$b=0.26\ \mathrm{Mpc}\,,$$

$$M_*(6.5\ \mathrm{Mpc})=2.92\times10^{15}\,M_\odot\,.$$

As a first approximation, we neglect the time variation of the total mass and of the density distribution of galaxies, and the self gravity of the injected gas. As mentioned above, it is beyond the aim of the present paper which mechanism of the injection is effective. We suppose that all the gas ejected from stars is added to the intracluster matter immediately. If the clusters are initially gas-free, the gas flowing out of galaxies by galactic winds accumulates so that ablation by ram pressure may become effective. We assume for simplicity that the gas is injected with zero relative velocity at the constant mass loss rate from galaxies.

Heat conduction should be taken into account in our interesting ranges of the temperature and the density. However, if there are some small scale magnetic fields such as those suggested from observations of the radio halo in the Coma cluster,[19] the conduction may be suppressed sufficiently. We then neglected it in the present study. In our calculations, we have taken the cooling by thermal bremsstrahlung into account. On these assumptions, we may write basic equations as follows:

$$\frac{\partial\rho}{\partial t}-\frac{1}{r^2}\frac{\partial}{\partial r}(r^2\rho u)=\alpha_s\rho_*(r)\,, \tag{3}$$

$$\rho\left(\frac{\partial u}{\partial t}+u\frac{\partial u}{\partial r}\right)+\alpha_s\rho_* u=-\frac{\partial P}{\partial r}-\rho G\frac{M_*(r)}{r^2}\,, \tag{4}$$

$$\frac{\partial(\rho\varepsilon)}{\partial t}+\frac{1}{r^2}\frac{\partial}{\partial r}(\varepsilon\rho u r^2)+\frac{P}{r^2}\frac{\partial}{\partial r}(ur^2)=\varepsilon_*\alpha_s\rho_*-Q\,, \tag{5}$$

where α_s denotes the specific rate of mass loss from galaxies, ε the specific internal energy of gas, ε_* the specific internal energy of the injected gas, and Q the cooling of thermal bremsstrahlung equal to $5\times10^{20}\rho^2T^{1/2}$ erg sec^{-1} cm^{-3}. We assume α_s and ε_* to be time-independent. The specific internal energies are given by

$$\varepsilon=3P/2\rho\,,\quad \varepsilon_*=3kT_*/m_\mathrm{H}\,, \tag{6}$$

where T_* denotes the temperature of the injected gas, m_H the hydrogen mass and others have usual meanings. We have assumed fully ionized pure hydrogen gas, that is,

$$P = 2k\rho T/m_H . \tag{7}$$

In order to show the characteristics of flows in clusters, we rewrite Eqs. (3) ~ (5) into a non-dimensional form. Since it takes the Hubble time, t_H, before the cooling becomes effective, the difference of physical quantities between the cases with and without cooling is as small as a few per cent. Thus, we ignore the term of cooling in the following discussion.

If the following non-dimensional variables are introduced,

$$\begin{aligned} &r' = r/b, \ t' = t/(b/c_0), \\ &\rho' = \rho/(\alpha_s \rho_*(0) b/c_0), \ u' = u/c_0, \ T' = T/T_*, \end{aligned} \tag{8}$$

where $c_0 = (10kT_*/3m_H)^{1/2}$, is the sound velosity, and if $Q=0$, we may rewrite Eqs. (3) ~ (5) as

$$\frac{\partial \rho'}{\partial t'} + \frac{1}{r^2}\frac{\partial}{\partial r'}(r'^2 \rho' u') = f(r'), \tag{9}$$

$$\rho'\left(\frac{\partial u'}{\partial t'} + u'\frac{\partial u'}{\partial r'}\right) + f(r')u' = -\frac{3}{5}\frac{\partial}{\partial r'}(\rho' T') - \Gamma g(r')\rho', \tag{10}$$

$$\frac{\partial}{\partial t'}(\rho' T') + \frac{1}{r'^2}\frac{\partial}{\partial r'}(r'^2 u' \rho' T') + \frac{2}{3}\frac{\rho' T'}{r'^2}\frac{\partial}{\partial r'}(r'^2 u') = f(r'). \tag{11}$$

Here we have a non-dimensional parameter

$$\Gamma = \frac{3GM_c/b}{c_0^2}, \tag{12}$$

and non-dimensional density and mass distributions

$$f(r') = 1/(1+r'^2)^{1.5}, \tag{13}$$

$$g(r') = [\ln\{r' + (1+r'^2)^{0.5}\} - r'/(1+r'^2)^{0.5}]/r'^2 . \tag{14}$$

It appears that if α_s is varied as $\beta\alpha_s$ under a given gravitational potential and a given T_*, the values of $\rho(r,t)$ and $P(r,t)$ become β times the original values, while $T(r,t)$ and $u(r,t)$ keep unchanged. Therefore, it is noted that the flow pattern of winds in clusters is determined by the parameter Γ which is a ratio of the central gravitational potential to the square of the sound velocity. The introduced non-dimensional parameters and variables are slightly different from those of Cowie and Perrenod,[15] because of different units. The scaling law reveals that the X-ray luminosity proportional to $\rho^2 T^{1/2}$ for thermal bremsstrahlung is transformed as α_s^2. This scaling law will be used in § 4.

We have coded a program in the spherical symmetric beam scheme[20] that the accuracy was verified for standard problems. The model cluster is initially gas-free and gas begins to be injected into the cluster. As inner boundary conditions, neither a sink nor a source is assumed. The velocity of gas at the center is set equal to zero, which differs from that of Lea[5] and Cowie et al.[15] The pressure and the density beyond the radius of the cluster $R=6.5$ Mpc are taken zero. It has been verified that the flow within $r=2$ Mpc and the X-ray luminosity is independent of the value of R. The space grid size Δr was uniformly taken 50 kpc, since the luminosity is sensitive to the value of Δr. Indeed, the total luminosity of X-rays for $\Delta r=100$ kpc decreased to a half of that for the case $\Delta r=50$ kpc, although the flow pattern was not changed.

In our calculations, a time-independent value of α_s is taken $3\times10^{-19}\,\mathrm{sec}^{-1}$ due to Huchtmeier et al.[21] Physical quantities for other values of α_s are able to be obtained by the use of the scaling law, because cooling is ineffective at the present cases. Thus, for the fixed values of α_s, b and $\rho_*(0)$, T_* remains as a parameter determining Γ. Since galaxies in a cluster move in high speed, the gas injected from them with zero velocity has kinetic energy corresponding to galactic dispersion velocity. The kinetic energy is transformed into thermal energy and T_* may be equal to the kinetic temperature of galaxies. According to Lea and De Young,[13] the temperature of gas stripped off from moving galaxies is about 10^6 °K or less, which is rather lower than currently expected values.

However, in order to study the effect of T_* upon the flow pattern, we take six spacially constant values of T_* as shown in Table I. In the last column of Table I, is added the case where T_* varies spacially. Taking account of the radial dependence of galactic dispersion velocity, $v_g(r)$, we reduce the kinetic temperature $T_*(r)=m_{\mathrm{H}}v_g^2(r)/6k$ from the tabulated data by King.[17] In this case, as the radius increases, the kinetic temperature decreases from 6.8×10^7 °K at the center to 2.3×10^7 °K at $R=6.5$ Mpc.

Table I. Computed results at nearly the Hubble time in a cluster of galaxies with the total mass of galaxies of $2.92\times10^{15}M_\odot$, and the core radius of galactic distribution of 0.26 Mpc.

T_* (°K)	10^6	5×10^7	10^8	2×10^8	3×10^8	4×10^8	$\propto v_g^2$
t ($\times10^{17}$sec)	3.1	3.0	3.2	3.0	3.0	3.1	3.0
Γ	606	12.12	6.06	3.03	2.01	1.53	—
r_{-} (Mpc)$^{a)}$	6.5	0.8	0.65	0.4	0.0	0.0	0.75
T_c ($\times10^8$ °K)	1.53	1.53	1.56	1.65	1.87	2.33	1.56
N_c ($\times10^{-3}\mathrm{cm}^{-3}$)	8.9	7.1	5.6	2.9	1.1	0.38	6.6
L_X ($\times10^{45}$erg/sec)	3.7	2.5	1.7	0.55	0.14	0.033	2.3
b_g (kpc)	356	358	366	368	429	500	363

a) radius of stagnation point.

§ 3. Numerical results and discussions

1) Flow patterns in clusters

The computed results at the Hubble time are given in Table I. It appears that the gas becomes pure inflow for the case $T_*=10^6$ °K ($\Gamma=6.06$). For inter-

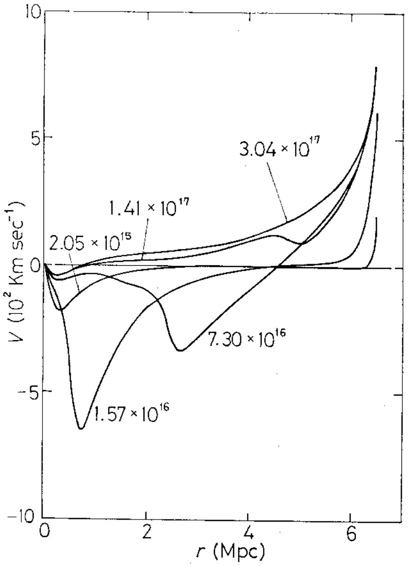

Fig. 1. Distribution of velocities for $T_*=5\times10^7$ °K. The time is labeled on curves in unit of seconds.

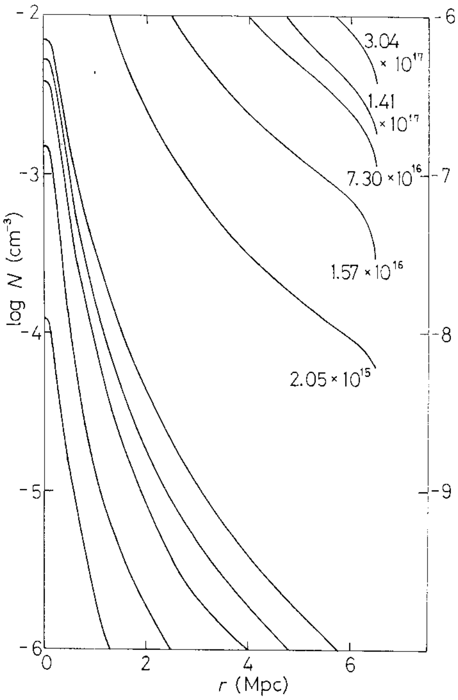

Fig. 2. Distribution of number densities for $T_*=5\times10^7$ °K. The time is labeled on curves in unit of seconds. Curves entering the top of the diagram refer to the scale on the right.

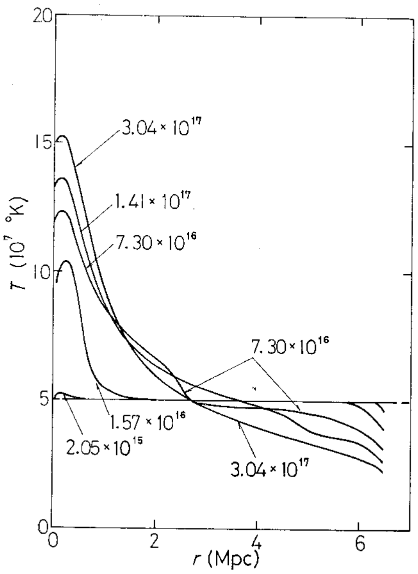

Fig. 3. Distribution of temperatures for $T_*=5\times10^7$ °K. The time is labeled on curves in unit of seconds.

mediate temperatures from 5×10^7 °K ($\Gamma=12.1$) to 2×10^8 °K ($\Gamma=3.03$), there is the stagnation point at the radius r_-, within which flow is inward, while the flow is outward outside of r_-. For the case $T_*=3\times10^8$ °K ($\Gamma=2.0$) or larger, we have wholly outward flows.

The time variations of velocity, density and temperature distribution for $T_*=5\times10^7$ °K are illustrated in Figs. 1, 2 and 3, respectively. The injected gas of $T_*=5\times10^7$ °K initially flows toward the center except the gas near the outer boundary and a compression wave propagates from the center. In the outer expanding region decreases the temperature of gas, while the temperature in the inflow region gradually increases due to adiabatic compression. Moving outwardly, the compression wave weakens, which reaches the outer boundary at $t\sim3\times10^{17}$ sec. The final velocity field of our runs for $T_*=5\times10^7$ °K shows that flow is inward within $r_-=0.8$ Mpc, whereas, outside of that value of r_-, outflow is realized with the velocity of a few 10 to 100 km sec^{-1}. The central temperature is increased up to $T_c\sim1.5\times10^8$ °K which is not enough to make flow outward. The density of gas is monotonically increased with time at all points. The total mass of injected gas till $t=3\times10^{17}$ sec amounts to $2.44\times10^{14}M_\odot$, most of which is retained in the cluster.

For the case of higher temperature $T_*=10^8$ °K, the flow is similar to that of $T_*=5\times10^7$ °K except weaker compression waves. For $T_*=2\times10^8$ °K, the gas initially expands against the gravitational field at the center where the pressure gradient is the steepest. The expansion of the gas in the central region forms a compression wave that propagates outwardly. At $t=4\times10^{16}$sec, the gas in the central region is cooled down to 1.45×10^8 °K due to adiabatic expansion and turns to infall. Thus, the central density is increased. At $t=t_{\rm H}$, the flow is inward within $r_-=0.4$ Mpc, while outward outside of r_-.

For the case $T_*=10^6$ °K, the gas injected from galaxies wholly accretes toward the center at the initial stage. After a bounce, a shock wave generates and propagates outwardly. The gas in the central region is heated up to $\sim10^8$ °K by the shock wave. At $t\sim10^{17}$ sec^{-1} when the shock front reaches at $r\sim2$ Mpc, the velocity of infalling gas before the front is about 1250 km sec^{-1}, while the velocity of the gas behind the front is 200 km sec^{-1}, which decreases toward the center. Thus, the gas heated up by the shock wave is successively warmed by adiabatic compression. At $t\sim3\times10^{17}$ sec, the shock wave arrives at $r=4.2$ Mpc and the gas flows inwardly as a whole. The velocities of the inflow before and behind the shock front are 700 and 200 km sec^{-1}, respectively. At this time, the central temperature reaches 1.5×10^8 °K. The central number density of the gas N_c is 9×10^{-3} cm^{-3}. Therefore, the cooling time ($\tau_c=3N_ckT_c/Q$) equals 4×10^{17} sec that is larger than the Hubble time and the cooling is ineffective even in this case.

In Figs. 4, 5 and 6, are shown the feature of the velocity, density and temperature distributions for 3×10^8 °K. Initially, the flow is similar to that in the

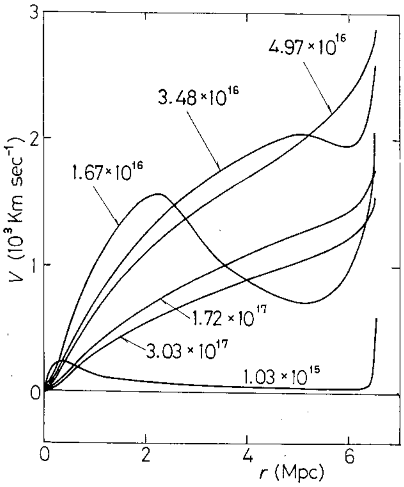

Fig. 4. The same as Fig. 1 but for $T_*=3\times10^8$ °K.

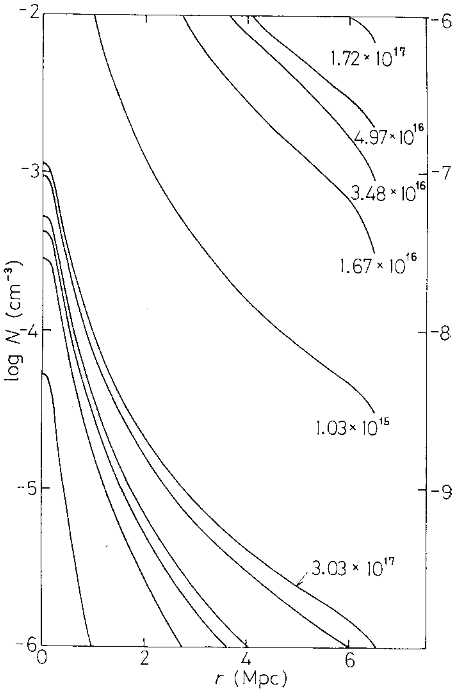

Fig. 5. The same as Fig. 2 but for $T_*=3\times10^8$ °K.

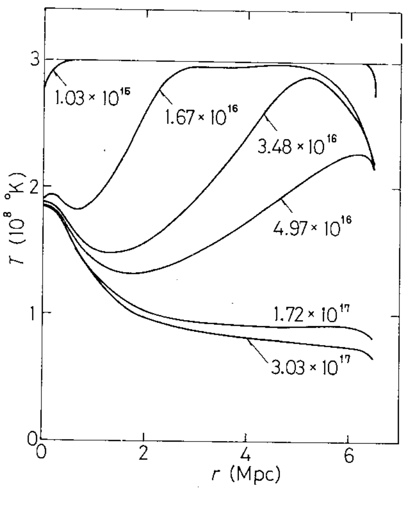

Fig. 6. The same as Fig. 3 but for $T_*=3\times10^8$ °K.

case $T_*=2\times10^8$ °K. A compression wave generates at the center, which moves outwardly and grows in strength until it reaches at the outer boundary. Then, the velocity of the gas gradually decreases due to the gravity, for instance at $r=5$ Mpc, from 2000 km sec^{-1} at $t=5\times10^{16}$ sec to 1000 km sec^{-1} at 3×10^{17} sec. Although the initial strong expansion results in the decrease of the temperature in the central region, the gas never turns to infall contrary to the case $T_*=2\times10^8$ °K. After $t\sim2\times10^{16}$ sec, the central temperature becomes nearly constant value of 1.8×10^8 °K, while the temperature in outer region decreases with time. The density increases monotonically at all regions in the cluster. The final central density of $N_c\sim10^{-3}$ cm^{-3} is seven times smaller than that for the case

$T_{*}=5\times10^{7}$ °K. The total mass of gas in the cluster is $1.3\times10^{14}\,M_{\odot}$. The velocity distribution for $T_{*}=4\times10^{8}$ °K is similar to that for $T_{*}=3\times10^{8}$ °K. The compression wave, however, reaches the outer boundary faster than in the lower T_{*} case and the pure outflow becomes nearly steady state at $t\sim1.5\times10^{17}$ sec. This seems to correspond to the steady solutions by Yahil and Ostriker.[14]

In Fig. 7, the time variation of T_c and N_c is shown. It is noted that N_c for $T_{*}=4\times10^{8}$ °K becomes constant with time and that the central temperature for the cases $T_{*}=10^{6}$, 5×10^{7} and 10^{8} °K is nearly the same value of 1.5×10^{6} °K in spite of the difference of T_{*}.

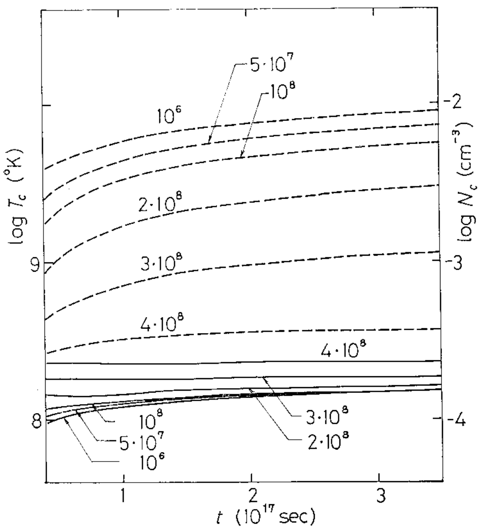

Fig. 7. Time variation of the central temperature and the central number density (dotted curves) for attached values of T_{*}.

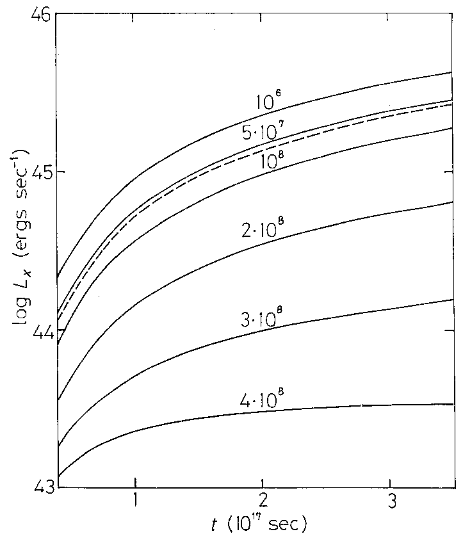

Fig. 8. Time-dependence of total X-ray luminosities for various values of T_{*}. The dotted curves denote the case where the temperature of injected gas decreases with the distance from the center.

2) X-ray luminosities

The time variation of total X-ray luminosity from the hot gas in the cluster due to thermal bremsstrahlung is shown in Fig. 8 for various values of T_{*}. It appears that as time increases, the luminosity increases smoothly and monotonically for all cases. The luminosity decreases as T_{*} is increased for a given mass loss rate. This is caused by the decrease of the central density due to the decrease of falling matter towards the center. For $T_{*}=4\times10^{8}$ °K, the curve becomes constant as the gas flows steadily. The curve is also given in Fig. 8 for the case where $T_{*}(r)$ varies spacially. It seems that the behavior of the X-ray luminosity is insensitive to the radial distribution of T_{*}.

The core radius of gas density distribution, b_g,[22] is evaluated and tabulated in the last line of Table I. For pure inflow and partial flow, b_g is approximately constant and small, while b_g increases for pure outflow as T_* increases.

3) Comparison with primordial gas infall models

The behavior of primordial infalling gas was studied by Lea and others.[6),15)] Hirayama[23)] computed the inflow of the primordial gas in the beam scheme method under the same values of $\rho_*(0)$, M_*, b and the same boundary conditions as in our calculations. The specific rate of mass loss from galaxies is equal to zero. At the initial time, the temperature and the density of initially homogeneous gas with zero velocity are taken as 10^6 °K and 10^{-29} g cm^{-3}, respectively. The density given here is that necessary to produce nearly the same total mass of gas in a cluster as that of gas after t_H for our case of mass injection from galaxies. According to Hirayama, as the primordial gas infalls, large gravitational energy is released at the center so that a strong shock wave generates and propagates with the velocity of several thousand km sec^{-1}. He obtained that at $t=t_H$, b_g equals 650 kpc, $T_c \sim 2.8\times10^8$ °K, $N_c \sim 2.5\times10^{-4}$ cm^{-3} and $L_X \sim 4\times10^{43}$ erg sec^{-1}. Since the central density and the X-ray luminosity depend upon the initial density of gas, these should not simply be compared with our case of mass injection. Because in the case of pure inflow and partial flow with mass injection, most of the gas is supplied at the central region where the density of galaxies is high, the gravitational energy released is smaller than in the case of the primordial gas distributed homogeneously at the initial time. Thus, the gas is piled up at the central region for our case. Moreover, the continuous injection of cooler gas from galaxies tends to decrease the central temperature. These seem to be the reason why T_c and b_g for our cases are smaller than those for the case of the primordial gas.

§ 4. Comparison with observations

The observational data of X-ray emissions from the Coma cluster[22)] indicate that the total X-ray luminosity L_X is 5×10^{44} erg sec^{-1}, the spectrum suggests the existence of a hot gas of 10^8 °K and b_g equal to 650 kpc.

We tabulate in Table II the values of the central number density and the corresponding mass loss rate which lead to the observed luminosity. These are obtained from Table I by using the scaling law that the velocity field, T_c and b_g are unchanged, if the cooling is ineffective. As a wide range of the mass loss rate is suggested between 10^{-18} and 10^{-20} sec^{-1},[9),24)] we cannot determine the unique

Table II. Central number densities and mass loss rates of models for observed total X-ray luminosity of 5.0×10^{44}erg sec^{-1}. The values of T_c and b_g are the same as those in Table I.

T_* (°K)	10^6	5×10^7	10^8	2×10^8	3×10^8	4×10^8	$\propto v_g^2$
N_c ($\times10^{-3}$cm^{-3})	3.3	3.2	3.0	2.8	2.1	1.5	3.1
α_s($\times10^{-19}$sec^{-1})	1.1	1.3	1.6	2.9	5.7	12	1.4

values of T_* and α_s from the observed X-ray luminosity.

For the case of the primordial gas, the central temperature is two times as large as the observed value and b_g agrees with that of the Coma cluster. Although b_g for pure outflow seems to agree with the observation, T_c is also higher. It should be noted that non-conductive pure inflow and partial flow of injected gas seem to account for the luminosity of X-rays, the gas temperature and the existence of the iron emission line in the Coma cluster. Although b_g is a factor of 2 smaller than the observation, further high resolution X-ray telescopes may improve them. For instance, Malina et al.[25] observed the core radius of 10′, that is, $b_g=0.4$ Mpc.

§ 5. Conclusion

We summarize the present arguments for the behavior of intracluster gas injected from galaxies in a cluster as follows.

(1) Under a gravitational field which is typified by the Coma cluster and a given mass loss rate, there are three flow patterns, depending on the temperature of the injected gas, at the Hubble time. For higher temperature than 3×10^8 °K, the gas flows wholly outwards and approaches a steady state within the Hubble time. The gas of lower temperature than 10^6 °K becomes pure inflow, while for intermediate temperatures, partial flow is appeared that the gas flows partially inwardly within a stagnation point and outwardly outside of it.

The central temperature for inflow and partial flow is 1.6×10^8 °K independent of the temperature of the injected gas at the Hubble time, while for pure outflow, it becomes higher than 1.6×10^8 °K as the temperature of the injected gas increases.

(2) Some of observational data of the Coma cluster, that is, the total X-ray luminosity, the temperature of a hot plasma, the core radius of the gas distribution and the existence of the iron emission line seem to be interpreted by pure inflow or partial flow of the injected gas.

(3) The pure inflow or partial flow model predicts rather a compact X-ray source than the primordial gas infall model and pure outflow model.

The iron emission line in X-rays from clusters shows that the chemical abundance of the hot gas is not equal to the cosmic abundance. This may mean that the hot gas is a mixture of the primordial gas and the injected gas from stars through galaxies. The flows of such a mixed gas are investigated by one of us (Y. H.) and will be published elsewhere.

Acknowledgements

The authors thank Professor Y. Ono, Professor S. Sakashita and Dr. N. Kaneko for fruitful discussions and encouragements. They are also grateful to Dr. F. Takahara and Dr. S. Ikeuchi for valuable discussions and informations on the work by Cowie et al. They would express their thanks to Professor R. Hoshi for his helpful comments. Numerical computations were carried out on a FACOM 230-75 at the Computer Center of Hokkaido University.

References

1) H. Gursky, E. Kellogg, S. Murray, C. Leong, H. Tananbaum and R. Giacconi, Astrophys. J. **167** (1971), L81.
E. Kellogg, H. Gursky, H. Tananbaum, R. Giacconi and K. Pounds, Astrophys. J. **174** (1972), L65.
W. Forman, E. Kellogg, H. Gursky, H. Tananbaum and R. Giacconi, Astrophys. J. **178** (1972), 309.
2) E. Kellogg, J. R. Baldwin and D. Koch, Astrophys. J. **199** (1975), 299.
A. Davidsen, S. Bowyer, M. Lampson and R. Cruddance, Astrophys. J. **198** (1975), 1.
A. Scheepmaker, G. R. Ricker, R. Brecher, S. G. Ryckman, J. E. Ballintine, J. P. Doty, P. M. Downey and W. H. G. Lewin, Astrophys. J. **205** (1976), L65.
3) R. J. Mitchell, J. L. Culhane, P. J. N. Davison and J. C. Ives, Month. Notices Roy. Astron. Soc. **176** (1976), 29.
P. J. Serlemitsos, B. W. Smith, E. A. Boldt, S. S. Holt and J. H. Swank, Astrophys. J. **211** (1977), L63.
4) S. F. Gull and K. J. E. Northover, Month. Notices Roy. Astron. Soc. **173** (1975), 585.
5) S. M. Lea, Astrophys. Letter **16** (1975), 141.
6) S. M. Lea, Astrophys. J. **203** (1976), 569.
F. Takahara, S. Ikeuchi, N. Shibazaki and R. Hoshi, Prog. Theor. Phys. **56** (1976), 1093.
7) P. R. Demarque and J. G. Mengel, Astrophys. J. **171** (1972), 583.
8) G. D. Coleman, Astrophys. J. **205** (1976), 475.
9) W. G. Mathews and J. C. Baker, Astrophys. J. **170** (1971), 241.
10) F. M. Ipavich, Astrophys. J. **196** (1975), 107.
11) H. E. Johnson and W. I. Axford, Astrophys. J. **165** (1971), 381.
12) J. E. Gunn and J. R. Gott, Astrophys. J. **176** (1972), 1.
G. Gisler, Astron. and Astrophys. **51** (1976), 137.
13) S. M. Lea and D. S. De Young, Astrophys. J. **210** (1976), 647.
14) A. Yahil and J. P. Ostriker, Astrophys. J. **185** (1973), 787.
15) L. L. Cowie and S. C. Perrenod, preprint.
16) L. L. Cowie and J. Binney, Astrophys. J. **215** (1977), 723.
17) I. R. King, Astrophys. J. **174** (1972), L123.
18) H. J. Rood, T. L. Page, E. C. Kinter and I. R. King, Astrophys. J. **175** (1972), 627.
19) M. A. G. Willson, Month. Notices Roy. Astron. Soc. **151** (1970), 1.
20) R. H. Sanders and K. H. Prendergast, Astrophys. J. **188** (1974), 489.
21) W. K. Huchtmeier, G. A. Tammann and H. I. Wendker, Astron. and Astrophys. **42** (1975), 205.
22) S. M. Lea, J. Silk, E. Kellogg and S. Murray, Astrophys. J. **184** (1973), L105.
23) Y. Hirayama, private communication.
24) J. S. Gallagher, Astron. J. **77** (1972), 568.
25) R. Malina, M. Lampton and S. Bowyer, Astrophys. J. **209** (1976), 678.